Strong Thermomechanical Squeezing via Weak Measurement

A. Szorkovszky,[1] G. A. Brawley,[1] A. C. Doherty,[2] and W. P. Bowen[1,*]

[1]*Centre for Engineered Quantum Systems, University of Queensland, St. Lucia 4072, Australia*
[2]*Centre for Engineered Quantum Systems, The University of Sydney, Sydney 2006, Australia*

(Received 25 January 2013; published 2 May 2013)

We experimentally surpass the 3 dB limit to steady-state parametric squeezing of a mechanical oscillator. The localization of an atomic force microscope cantilever, achieved by optimal estimation, is enhanced by up to 6.2 dB in one position quadrature when a detuned parametric drive is used. This squeezing is, in principle, limited only by the oscillator Q factor. Used on low temperature, high frequency oscillators, this technique provides a pathway to achieve robust quantum squeezing below the zero-point motion. Broadly, our results demonstrate that control systems engineering can overcome well established limits in applications of nonlinear processes. Conversely, by localizing the mechanical position to better than the measurement precision of our apparatus, they demonstrate the usefulness of mechanical nonlinearities in control applications.

DOI: 10.1103/PhysRevLett.110.184301 PACS numbers: 45.80.+r, 05.40.−a

High-quality mechanical oscillators are widely used for weak force detection [1,2], nanoscale manipulation [3,4], and quantum state engineering [5,6]. Such applications often utilize optimal estimation to localize the oscillator, followed by feedback control to confine its position. In a classical context, this type of control is commonly used to linearize the response of sensors driven into their nonlinear regime, resulting in increased dynamic range and suppression of resonance frequency fluctuations [7]. Furthermore, spurred by the growing prospect of accessing new quantum physics [8], similar techniques are now being applied to state-of-the art mechanical oscillators to cool them close to the quantum limit set by mechanical zero-point motion [9,10], and ultimately surpass it via quantum control techniques such as backaction evasion [11–13]. However, the level of achievable oscillator localization has always previously been limited to at best the measurement precision, presenting a significant barrier to applications in both quantum and classical regimes.

Applications of mechanical oscillators can also benefit from nonlinearities without requiring any measurement. An example of particular relevance to this Letter is mechanical parametric amplification, where direct modulation of the spring constant induces amplification of in-phase motion [14]. This technique is often used in microelectromechanical (MEMS) and nanoelectromechanical systems to boost mechanical signals from in-phase forces above the measurement noise floor [15,16]. Conversely, out-of-phase motion is deamplified and thereby more strongly confined or ''squeezed.'' In principle, squeezing below the zero-point motion variance V_g is possible. Such ''quantum squeezing'' has applications in quantum metrology and tests of macroscale entanglement and quantum gravity [8]. However, the emergence of mechanical instability limits the improvement in confinement to at most 50% (or −3 dB) in the steady state [17]. Since a mean thermal occupancy of just half a phonon increases the oscillator's motional variance to twice the zero-point motion variance, the 3 dB limit imposes a strict precooling requirement for quantum squeezing by this method. For typical micro- and nanomechanical oscillators with resonance frequencies in the range of 1–100 MHz, this temperature bound lies between 0.05 and 5 mK, outside the range of most conventional cryogenic setups.

Here, we combine control techniques and parametric modulation to both break the 3 dB limit for the first time and achieve mechanical localization exceeding the measurement sensitivity of our apparatus by 6.2 dB. The key concept, proposed recently in Ref. [17], is to induce correlations between the amplified and squeezed motional quadratures by detuning the parametric modulation. Information encoded on the amplified quadrature then allows the squeezed quadrature to be estimated with enhanced precision. Our experiments are performed with a conventional AFM cantilever at room temperature, and as such are far from the quantum regime. The enhanced localization possible through such ''thermomechanical squeezing'' can, however, be useful in force measurement, for instance, by increasing the dynamic range when signal distortion is introduced at large amplitudes [7,18], by broadening the bandwidth in the squeezed quadrature [19], and by enhancing the sensitivity to pulsed forces with known timing [20,21]. Furthermore, since the technique demonstrated here applies equally to quantum zero-point noise, it provides a path towards precise quantum control and robust quantum squeezing of mechanical oscillators at attainable temperatures and in the absence of strong measurement [17].

The experimental setup, shown in Fig. 1(a), is based on a commonly used optical measurement of the mechanical element in a typical MEMS. The position of a gold-coated AFM cantilever is monitored using a Mach-Zender

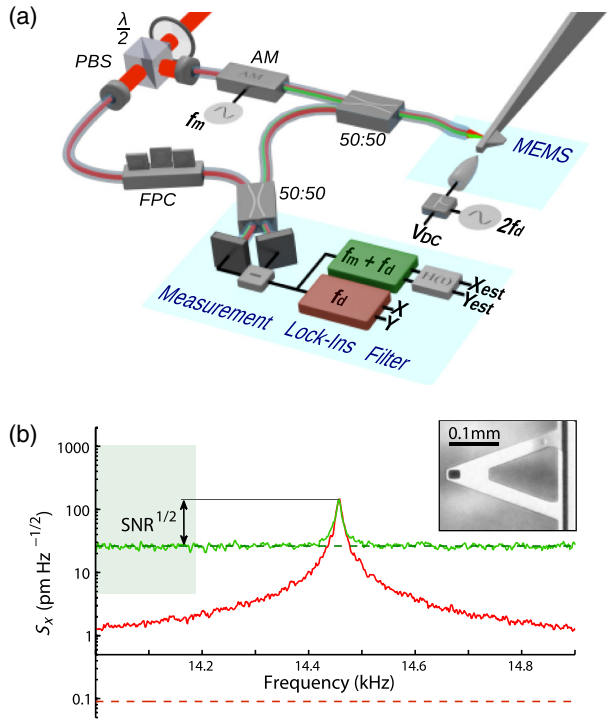

FIG. 1 (color online). (a) Schematic of the experimental setup. The dark gray (red) path in the fiber-based interferometer denotes the high-fidelity carrier signal while the light gray (green) path denotes the low-fidelity signal created by amplitude modulation (AM). PBS, polarizing beam splitter; FPC, fiber polarization controller. (b) Displacement noise spectrum around the fundamental cantilever resonance measured by the laser carrier [dark gray (red) line] and by the sideband created with a 1 V_{pp} modulation [light gray (green) line]. Dotted lines represent the respective shot-noise-limited sensitivities of the measurements, while the light gray (green) band corresponds to the range of sensitivity available from the sideband. Inset: Micrograph of the AFM cantilever used in this experiment.

interferometer in a balanced homodyne configuration, with a fiber tip used to focus the optical field onto the cantilever. The sensitivity S_x of the interferometer is 90 fm/$\sqrt{\text{Hz}}$, as shown in Fig. 1(b). This allows a high-fidelity measurement of the thermal noise in the fundamental mode of the cantilever, which is used to characterize its motion and the accuracy of our estimation procedure. The measurement noise for this signal $V_{\text{meas}} = 4\gamma S_x^2$, where γ is the mode's decay rate, is 60 dB below the thermally induced variance V_T. A weak sideband is also created using an intensity modulation of the bright field, providing a low-fidelity measurement with independent shot-noise characteristics which was used to perform position estimation. The sensitivity of this measurement could be varied between 25 and 1000 pm/$\sqrt{\text{Hz}}$ by adjusting the optical modulation depth, as illustrated in Fig. 1(b). At room temperature, the thermal noise signal lies within this region, allowing the study of estimation techniques in the important regime where the signal level is comparable to the measurement noise floor, i.e., where the signal-to-noise ratio (SNR) $= V_T/V_{\text{meas}} \approx 1$.

Parametric amplification requires the spring constant of the oscillator to be modulated near twice the resonance frequency f_0. For our cantilever, the spring constant was increased well above its intrinsic value $k_0 \approx 0.06$ N/m by applying 450–650 V between the cantilever and a nearby electrode, an effect due to the nonlinear position dependence of capacitive energy in this geometry [14]. Since the frequency shift is proportional to the square of the voltage, this dc offset increases the peak-to-peak frequency modulation χ of the oscillator's fundamental mode from an additional alternating voltage [15]. The position measurements were fed into lock-in amplifiers with a bandwidth much wider than the mechanical decay rate γ, allowing the position dynamics around f_0 to be observed in a rotating frame at a nearby reference frequency $f_d = f_0 + \Delta$. The lock-in outputs X and Y, describing orthogonal quadrature components of the position $x = X\cos(2\pi f_d t) + Y\sin(2\pi f_d t)$, allow easy visualization of the amplitude and phase of oscillation. The parametric effect from an alternating voltage at frequency $2f_d$ applied between the electrode and the cantilever leads to a preferred phase of mechanical oscillation and hence a squeezed thermal distribution in the X-Y plane.

Initially, the high-fidelity measurement was used to analyze above- and below-threshold position statistics under parametric amplification. Here, the dc voltage was set to 450 V, shifting the fundamental mode frequency f_0 from 9.6 to 12.5 kHz. When driven on resonance ($\Delta = 0$), and with a strength above the instability threshold ($\chi > \gamma$), thermomechanical squeezing surpasses 3 dB while the orthogonal quadrature is amplified indefinitely. Figure 2(a) shows the time evolution of the maximally squeezed and antisqueezed quadrature variances measured in this regime, with $\chi = 22.5$ Hz and $\gamma = 2$ Hz. Good agreement with theory is observed at short times (<20 ms) during which the squeezing approaches 11 dB. However, the amplified quadrature saturates after approximately 35 ms, when the amplitude approaches the optical quarter-wavelength of 195 nm and oscillations are no longer confined to the linear portion of the interference fringe. Crucially, a side effect of this measurement nonlinearity is a severe degradation in observed squeezing well before saturation is apparent. Such limits to dynamic range therefore preclude the generation of all but transient squeezing above threshold. Nonetheless, the strong squeezing observed reproduces the nonequilibrium squeezing observed in trapped ions [22] for the first time in a micromechanical oscillator, albeit in the classical regime. Transient squeezing of this kind could be useful in applications where operation outside of equilibrium is acceptable, such as stroboscopic sensing [20].

By detuning the parametric drive off resonance, the oscillator phase undergoes a net rotation with respect to the amplification axis, increasing the instability threshold

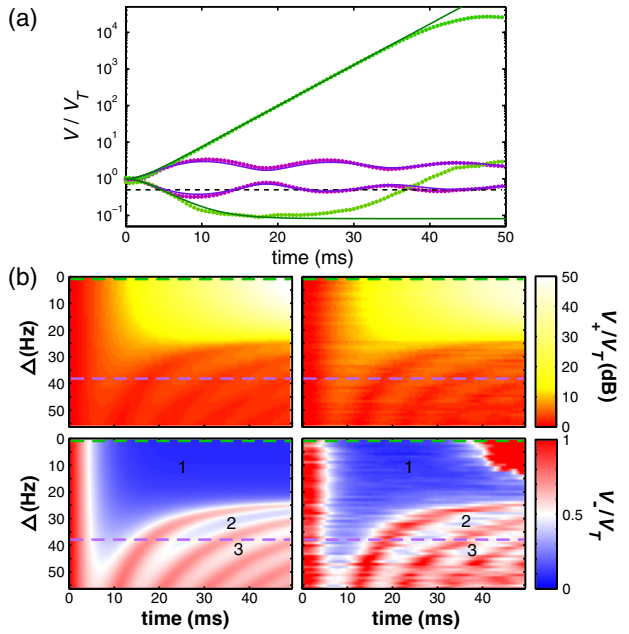

FIG. 2 (color online). Evolution of the squeezed and anti-squeezed quadratures with a continuous parametric drive of strength $\chi = 22.5$Hz turned on at $t = 0$. (a) Normalized quadrature variances versus time for an on-resonance drive [light gray (green) line] and for a below-threshold detuned drive with $\Delta = 38$ Hz [dark gray (violet) line]. Solid lines are theoretical fits, while points show experimental statistics generated from 200 iterations of the drive turn-on. The dotted line represents the -3 dB steady-state squeezing limit. At each point in time, the quadratures are rotated so that the covariance $\langle XY\rangle - \langle X\rangle\langle Y\rangle \approx 0$ over all iterations. A ring-up time of 2.5 ms is chosen for the parametric drive to minimize impulse forces on the cantilever. (b) Theoretical (left) and experimental (right) variances as a function of detuning and time. Numbered grey (blue) areas indicate squeezing below 3 dB.

to $\chi_{\text{th}} = \sqrt{\Delta^2 + \gamma^2}$ [23]. Consequently, for the drive strength used here ($\chi = 22.5$ Hz), the oscillator is unstable for detunings below $\Delta = 22.4$ Hz. When the detuning is increased further so that $\Delta > \chi$, the phase-space trajectories form stable elliptical orbits. The variances initially mirror this oscillatory behavior before relaxing to steady-state values in the long time limit, in quantitative agreement with theoretical modeling [23]. The effect of increasing detuning on the transient statistics can be seen in Fig. 2(b), where a dramatic change from monotonic behavior to clear oscillations in the variance occurs at the threshold detuning. Notably, transient squeezing below 3 dB is still possible below threshold, owing to the rapid drive turn-on. The final steady-state variances can be expressed with respect to the thermal variance V_T as $V_\pm/V_T = (1 \mp \chi/\chi_{\text{th}})^{-1}$ [23]. The squeezing limit of $V_T/2$ is therefore—while not a constraint outside of equilibrium—a fundamental one when in the steady state.

From the above observations, the benefit of a parametrically driven system in equilibrium would appear to be limited to enhanced readout in one quadrature and 3 dB reduced variance in the other. However, it has been recently predicted that these phenomena can be combined to enhance localization using a weak measurement and optimal estimation [17]. For an oscillator detuned so that $\Delta > \chi$ and which has relaxed to the steady state, the thermally excited oscillations will alternate between amplified and squeezed quadratures before decaying. Since the dynamics of the system are well known, a measurement of the amplified quadrature will provide some capacity to estimate the squeezed quadrature at a later time. The squeezed quadrature therefore obtains an effective sensitivity enhancement without amplifying its mechanical fluctuations. This is useful for localizing an oscillator where conditions such as cold environment, poor measurement sensitivity, or high oscillator frequency limit the SNR.

Using control theory, the filter that extracts the best quadrature estimates from noisy measurements can be written in terms of parameters defining the oscillator's expected time evolution along with the measurement sensitivity [23]. For an oscillator with no parametric drive, the optimal quadrature estimates X_{est} and Y_{est} that be obtained from the low-fidelity measurement records $\tilde{X}$ and $\tilde{Y}$ are of the form $X_{\text{est}}(t) = g_0 \int_0^t \tilde{X}(\tau) e^{-\Gamma_0(t-\tau)} d\tau$ and $Y_{\text{est}}(t) = g_0 \int_0^t \tilde{Y}(\tau) e^{-\Gamma_0(t-\tau)} d\tau$. With a detuned parametric drive turned on, the two quadratures become correlated and the estimates require a more complex convolution [23], the implementation of which is described in the Supplemental Material [24]. The best effective localization of the oscillator from these estimates can be quantified using conditional variances. For example, the conditional X quadrature variance V_X is the mean square of the residual noise $X(t) - X_{\text{est}}(t)$. The conditional variance also defines the minimum effective temperature of a quadrature achievable from ideal feedback cooling, equivalent to applying phase-space displacements in the X and Y quadratures by X_{est} and Y_{est}, respectively, over time, as illustrated in Fig. 3(a).

Steady-state estimation was performed with the cantilever tuned to 14.5 kHz by a 650 V bias and varying the sideband intensity to tune the SNR of the low-fidelity measurement. For each SNR, continuous low-fidelity measurements of the two quadratures of cantilever motion were recorded in both the undriven case and with an applied parametric drive of strength $\chi = 57$ Hz and detuning $\Delta = 63$ Hz to ensure the below-threshold condition. In both cases, optimal estimates X_{est} and Y_{est} were generated in postprocessing by minimizing the respective conditional variances over the filter parameters. Phase-space Brownian trajectories $\{X, Y\}$ determined from the high-fidelity measurement are plotted in Fig. 3(b), along with corresponding residual noise $\{X - X_{\text{est}}, Y - Y_{\text{est}}\}$ after applying the optimized filter to the low-fidelity measurements in the low, intermediate, and high SNR regimes. As expected, when no parametric drive is applied, the quadratures of motion

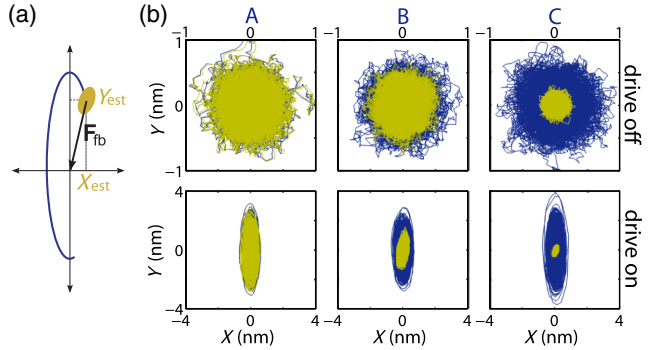

FIG. 3 (color online). Reducing variance via estimation. (a) Typical phase-space trajectory over a short time with a detuned parametric drive applied to the oscillator. The estimates $\{X_{\mathrm{est}}, Y_{\mathrm{est}}\}$ at a given time agree with a high-fidelity measurement (blue curve) to within an uncertainty given by the yellow ellipse, localizing the oscillator to this phase space region. A feedback force $\mathbf{F}_{\mathrm{fb}}$ confining the oscillator to near the origin can be modeled by subtracting the estimates from the high-fidelity data. (b) Quadrature phase-space trajectories for 22.5 second samples obtained from high-fidelity measurement [dark (blue)] and the residual after subtracting the estimate [light (yellow)]. The upper panels show the random-walk pattern in the undriven case mixed down at the resonance frequency for weak (A), intermediate (B), and strong measurement (C). The lower panels show the elliptical trajectories and residual noise for a parametric drive strength of $\chi = 57$ Hz detuned close to threshold and using the same SNR as above.

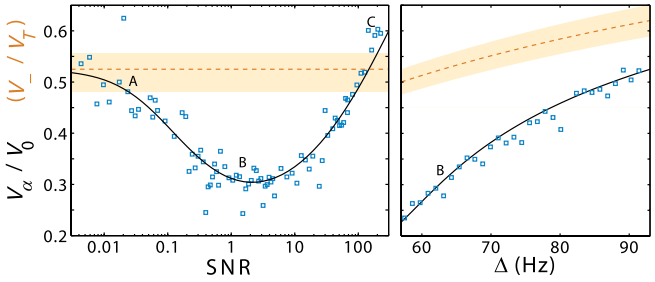

FIG. 4 (color online). Steady-state squeezing ratios plotted against SNR for $\Delta = 63$ Hz (left) and against detuning for SNR ≈ 1 (right). Squares show the squeezing ratio for each combination of experimental parameters, with theoretical fits shown as solid lines. Dotted curves are fits to the squeezing without estimation, limited to $1/2$, with shaded bands to represent the experimental error margin. Labels A–C indicate the data points used to generate the trajectories in Fig. 3.

have equal uncertainty, determined by the optimal conditional variance; i.e., $V_X = V_Y = V_0$. As the thermal signal increases towards the noise floor (SNR approaches 1), the conditional variances drop sharply as expected. At maximum sideband intensity, the rms uncertainty in both quadratures is reduced from the thermal value of 240 to 60 pm, corresponding to an effective temperature decrease from 300 to 19 K. With the drive turned on, the high-fidelity measurement shows unconditional thermomechanical squeezing close to, but not surpassing, the 3 dB limit. Critically, elliptical trajectories can be observed, establishing the correlations required for our estimation protocol between squeezed and antisqueezed quadratures. After subtracting the optimal estimate, the residual noise is maximally squeezed at an angle α that increases with SNR. The variance V_α of this quadrature decreases monotonically along with the antisqueezed variance as the measurement improves, with the residual noise becoming symmetric in the high SNR limit.

The squeezing ratio V_α/V_0 determined from this analysis is shown in Fig. 4 as a function of SNR, agreeing well with theory. As expected, the variances reproduce the unconditional squeezing in the weak measurement limit and the parametric drive has no effect in the strong measurement limit. However, in the intermediate regime where SNR ≈ 1 there is a distinct minimum, allowing enhanced localization and breaking the 3 dB limit by a significant factor. As can be seen in Fig. 4 (right), the squeezing can be improved further by adjusting detuning closer to threshold, with a maximum thermomechanical squeezing of 6.2 dB achieved. These results can be understood by the fact that the effective increased sensitivity due to the parametric drive is of greatest benefit near the noise floor and with maximal amplification of the orthogonal quadrature. Since the maximum squeezing is proportional to $\sqrt{\chi/\gamma}$ [23], it can be enhanced by increasing the parametric drive strength, subject to the condition $\chi \ll f_0$. In principle, this allows arbitrary suppression of one quadrature of motion, exceeding the usual limit for control systems defined by the measurement precision. For applications requiring confinement in addition to localization, optimal estimates must be calculated in real time in order to be fed back as a damping force. As shown here by optimization, this can be achieved by using the well-defined filter parameters in Ref. [23].

Although demonstrated with thermal fluctuations, our technique applies in the same manner to the zero-point motion of an oscillator, with the maximum reduction in conditional variance V_α/V_0 independent of temperature [23]. The effect of the quantum modification at low temperatures—known as backaction noise—is instead to limit the initial conditional variance V_0 to be no lower than the ground state variance. Therefore, our approach could enable strong quantum squeezing and ultraprecise quantum control [25]. Experiments with sensitivity near the standard quantum limit (where SNR ≈ 1 at zero temperature) have been performed recently with mechanical oscillators [13,26]. While purely measurement-based schemes exist to create mechanical squeezed states [11,12], significant squeezing requires high measurement strengths and efficiencies yet to be demonstrated in mechanical oscillators. Nanoelectromechanical systems are, however, commonly integrated with a parametric drive [15,16] and can be precooled to near the ground state [27,28]. Such emerging systems are therefore good candidates for quantum

squeezing using our technique, even without significant advances in transduction.

We have observed parametric thermomechanical squeezing of a micromechanical oscillator exceeding 3 dB for the first time, both transient and in equilibrium, with the latter breaking a well-known limit for parametrically driven systems. This result demonstrates that the 3 dB limit to steady-state parametric squeezing is not fundamental, and facilitates the wider use of thermomechanical squeezing in control and sensing applications. The combination of parametric driving, measurement, and estimation sheds light on the important interface between quantum measurement and control that is being approached most notably in opto- and electromechanical systems. The techniques introduced, if applied in conjunction with state-of-the-art readout techniques and high quality oscillators, also open the door for the engineering of nonclassical states of mesoscopic mechanical systems. More broadly, our results demonstrate that combining oscillator nonlinearity with control can both overcome fundamental limitations on parametric processes and localize mechanical motion beyond constraints imposed by the measurement sensitivity.

This research was funded by the Australian Research Council Centre of Excellence CE110001013 and Discovery Project DP0987146.

*wbowen@physics.uq.edu.au

[1] C. L. Degen, M. Poggio, H. J. Mamin, and D. Rugar, Phys. Rev. Lett. **100**, 137601 (2008).
[2] P. Verlot, A. Tavernarakis, C. Molinelli, A. Kuhn, T. Antoni, S. Gras, T. Briant, P.-F. Cohadon, A. Heidmann, L. Pinard, C. Michel, R. Flaminio, M. Bahriz, O. L. Traon, I. Abram, A. Beveratos, R. Braive, I. Sagnes, and I. Robert-Philip, C. R. Physique **12**, 826 (2011).
[3] S. C. Masmanidis, R. B. Karabalin, I. De Vlaminck, G. Borghs, M. R. Freeman, and M. L. Roukes, Science **317**, 780 (2007).
[4] D. R. Koenig, E. M. Weig, and J. P. Kotthaus, Nat. Nanotechnol. **3**, 482 (2008).
[5] A. D. O'Connell, M. Hofheinz, M. Ansmann, R. C. Bialczak, M. Lenander, E. Lucero, M. Neeley, D. Sank, H. Wang, M. Weides, J. Wenner, J. M. Martinis, and A. N. Cleland, Nature (London) **464**, 697 (2010).
[6] J. D. Teufel, T. Donner, D. Li, J. W. Harlow, M. S. Allman, K. Cicak, A. J. Sirois, J. D. Whittaker, K. W. Lehnert, and R. W. Simmonds, Nature (London) **475**, 359 (2011).
[7] D. Hall and A. Flatau, J. Sound Vib. **211**, 481 (1998).
[8] M. Blencowe, Phys. Rep. **395**, 159 (2004).
[9] M. Poggio, C. L. Degen, H. J. Mamin, and D. Rugar, Phys. Rev. Lett. **99**, 017201 (2007).
[10] D. Kleckner and D. Bouwmeester, Nature (London) **444**, 75 (2006).
[11] A. A. Clerk, F. Marquardt, and K. Jacobs, New J. Phys. **10**, 095010 (2008).
[12] M. R. Vanner, I. Pikovski, G. D. Cole, M. S. Kim, Č. Brukner, K. Hammerer, G. J. Milburn, and M. Aspelmeyer, Proc. Natl. Acad. Sci. U.S.A. **108**, 16 182 (2011).
[13] J. B. Hertzberg, T. Rocheleau, T. Ndukum, M. Savva, A. A. Clerk, and K. C. Schwab, Nat. Phys. **6**, 213 (2009).
[14] D. Rugar and P. Grütter, Phys. Rev. Lett. **67**, 699 (1991).
[15] Q. P. Unterreithmeier, E. M. Weig, and J. P. Kotthaus, Nature (London) **458**, 1001 (2009).
[16] J. Suh, M. D. LaHaye, P. M. Echternach, K. C. Schwab, and M. L. Roukes, Nano Lett. **10**, 3990 (2010).
[17] A. Szorkovszky, A. C. Doherty, G. I. Harris, and W. P. Bowen, Phys. Rev. Lett. **107**, 213603 (2011).
[18] V. Natarajan, F. DiFilippo, and D. E. Pritchard, Phys. Rev. Lett. **74**, 2855 (1995).
[19] J. Mertz, O. Marti, and J. Mlynek, Appl. Phys. Lett. **62**, 2344 (1993).
[20] D. Vitali, S. Mancini, L. Ribichini, and P. Tombesi, Phys. Rev. A **65**, 063803 (2002).
[21] D. Weld and A. Kapitulnik, Appl. Phys. Lett. **89**, 164102 (2006).
[22] D. M. Meekhof, C. Monroe, B. E. King, W. M. Itano, and D. J. Wineland, Phys. Rev. Lett. **76**, 1796 (1996).
[23] A. Szorkovszky, A. Doherty, G. Harris, and W. Bowen, New J. Phys. **14**, 095026 (2012).
[24] See Supplemental Material at http://link.aps.org/supplemental/10.1103/PhysRevLett.110.184301 for full description of the filter and postprocessing method.
[25] H. M. Wiseman and G. J. Milburn, Phys. Rev. A **49**, 1350 (1994).
[26] A. Schliesser, O. Arcizet, R. Riviere, G. Anetsberger, and T. J. Kippenberg, Nat. Phys. **5**, 509 (2009).
[27] B. H. Schneider, S. Etaki, H. S. J. van der Zant, and G. A. Steele, Sci. Rep. **2**, 599 (2012).
[28] R. B. Karabalin, X. L. Feng, and M. L. Roukes, Nano Lett. **9**, 3116 (2009).